Paper No.
08308

NACE INTERNATIONAL CORROSION 2008 CONFERENCE & EXPO

MODELING OF POLARIZATION BY POINT ANODES FOR PREVENTION OF REINFORCING STEEL CORROSION

M. Dugarte*+, A.A. Sagüés*
* Department of Civil and Environmental Engineering, University of South Florida,
4202 East Fowler Ave., Tampa, FL 33620, U.S.A.
+ On leave from: Universidad del Norte, Barranquilla, Colombia.

R. G. Powers
Materials Office, Florida Department of Transportation,
5007 NE 39th Ave., Gainesville, FL 32602, U.S.A

ABSTRACT

This paper addresses the first phase in developing a numerical model for polarization distribution prediction of the rebar-anode system in reinforced concrete slabs with residual chloride contamination, where sacrificial point anodes were embedded in the concrete patch repair area. The modeling approach was developed to characterize the performance of this system under two application scenarios: one with part of the rebar assembly in the active condition and the other with an all-passive assembly. The model results and experimental findings in > 2 year old concrete slabs are compared. Results could be used to determine the anode operating potentials that may be achieved with specific anode placement spacing for highway applications. Experimental polarization curves provide additional information for future modeling improvement.

Key Words: anodes, zinc, cathodic protection, concrete, corrosion, reinforcing steel.

INTRODUCTION

Small anodes are commercially available to be cast in patch repairs of concrete, to prevent the initiation of “halo effect” corrosion on the rebar in areas around the patch with residual high chloride content. The anodes have a zinc alloy piece embedded in a mortar disk with connecting wires. The mortar around the zinc alloy has admixtures that promote high pH or otherwise activate the zinc, and also may contain humectants [1-4].

In the present ongoing investigation two types of anodes were evaluated in reinforced concrete slabs configurations to permit determination of protective current distribution over a uniform reinforcing bar array. The results were used to formulate a model of the combined polarization performance of the anodes and rebar toward establishing predictive methods for quantifying throwing power in situations representative of highway applications.

This work reviews also the data associated with anode polarization performance in laboratory controlled humidity chambers [5]. At the end comparisons between laboratory and slab system installations are presented.

EXPERIMENTAL PROCEDURE

Specimens and Materials

Six test reinforced concrete slabs with dimensions 4 ft long, 1.5 ft wide and ½ ft thick (1.2 m x 0.45 m x 0.15 m) were constructed. Each slab contains 12 embedded segments of #7 bars (2.2 cm nominal diameter) of plain steel rebar placed ladder-wise at equal intervals, 4 in. (10 cm) apart, spanning the length of each slab. The schematic of the specimen is shown in Figure 1. The slabs were built using Ordinary Repair Concrete (Table 1), except that the shaded portion near the center contained admixed NaCl to obtain 6 Kg/m^3 chloride ion simulating a conventional patch repair case. Four bars were located near the center of the slab, in contact with chloride contaminated concrete, resulting in an active - net anode condition. The remaining rebars were passive.

Galvanic, zinc alloy point anodes were placed between bars No. 4 and No. 5 and connected to the rest of the rebar assembly in each test slab. Two anode types were used and designated as follows: Type C (triplicate slabs numbered 1, 3 and 5) or Type W (triplicate slabs 2, 4 and 6). Both Type C and W anodes were made of zinc alloy anode embedded in pellet of mortar with zinc alloy mass of ~ 30 g and mortar pellet external diameter (or side dimension if approximately square) ~70 mm and thickness ~30 mm. For type C, the anode was embedded in highly alkaline mortar and for type W, the anode was embedded in mortar with humectants and proprietary zinc activators.

The slabs were cast and kept curing in the molds for 7 days, then the slabs were demolded and placed horizontally, elevated 1 ft above ground, in an outdoor test yard ~ 20 km inland from Tampa Bay in Florida. The main anode was kept provisionally wired to the four rebars in the Cl- rich zone while still curing in the forms and connected to the entire rebar assembly at 7 days which was designated as the start of the exposure period (t=0).

Additional experiments were performed with anodes embedded in concrete specimens with dimensions 20 cm x 20 cm x 10 cm, with no reinforcement, but fitted with a counter and an activated titanium rod (ATR) reference electrode[5]. The concrete specimens were built using the same Ordinary Repair Concrete formulation as for the concrete slabs. These specimens were subjected to anodic galvanostatic polarization at 30, 100 and 300 □A as well as open circuit conditions. The specimens were exposed to a relative humidity of 95%. The potential evolution of the anodes thus exposed was monitored for 900 days. Details of the experimental arrangement are given in Reference [5].

Resistance and Electrochemical Measurements

Nominal concrete resistance measurements were performed periodically between consecutive rebar segments. An activated titanium reference electrode was placed next to each rebar to perform potential measurements. A copper/copper sulfate electrode (CSE) was used to measure the potential of each segment with respect to the concrete next to each rebar. All rebars were normally interconnected with external wiring and switches that allowed measuring the macrocell current delivered/received by each bar segment and performing depolarization tests. Monitoring measurements were performed periodically over 2.5 years including the anode current and the instant off potential as the corrected potential in which a voltage drop in the concrete is disconnected. The anode on the slab centerline (Main) was always connected to the rest of the rebar assembly. The other anode (Auxiliary) was disconnected except for special tests. The slabs were maintained outdoors under normal ambient exposure and the air temperature was recorded.

The current delivered by the anodes to the entire rebar assembly as function of exposure time is shown in Figure 2. Initial currents were in the order of 1-3 mA but after 1020 days current from the C and W anodes had dropped to ~200 μA and 30 μA respectively. Potential and current distribution patterns along the slab (see Results section) showed that rebars in the chloride-contaminated zone were mostly net anodes, contributing often a total anodic current comparable to or exceeding the current supplied by the point anode. The rebar potential distribution along the slab main direction showed clearly that the main polarizing sources of the rest of the system were the rebars in the chloride contaminated zone, which exhibited potentials typical of actively corroding steel. After the rebars in the chloride zone were disconnected (day 477), the decreasing current trend was arrested or even reversed for both anodes. Thereafter, the anodes were the most negative elements in the system, and the only source of cathodic polarization of the remaining, passive, bars.

Four-hour depolarization test results are shown in Figures 3 and 4. These figures show the polarization achieved in rebar segments 1-5 (Figure 1), using the average values for rebar pairs 1-2, 2-3, 3-4 and 4-5, which are closest to the anode and all in the passive condition, averaging in turn results from the triplicate test slabs. For the period before disconnection of the active rebars, depolarization tended to be greater at the bars further removed from the anode (e.g. 1-2), but that was an effect of the presence of the active rebars on the overall macrocell relaxation during depolarization. After the active bars were permanently disconnected, the expected trend of less polarization further away from the anode was observed. The extent of depolarization after ~100 days was significantly greater for the C anodes than for the W anodes, consistent with the difference in overall current levels evident in Figure 2. However, during the period when all rebars were connected, not even the C anodes achieved depolarization levels reaching 100 mV.

Upon disconnection of the active rebars the maximum average depolarization increased significantly (up to ~140 mV) for the C anodes and slightly for the W anodes, reflecting the removal of the less polarizable, lower potential active steel. However, there was a subsequent decay. The level of depolarization achieved by 1020 days even for the C anodes was again less than 100 mV despite that only the small passive steel area was being polarized.

MODELING

The slab was idealized as consisting of several discrete steel segments in concrete, as shown in Figure 5 and following the approach in References [6] and [7]. Active rebar elements were treated as the combination of a cathodic and an anodic element separated by a small resistance. The other elements were separated by resistors corresponding to the resistance of the concrete slice between elements. The model input consists of the polarization parameters for each of the anodic and cathodic reactions (cathodic Tafel slope, pseudoexchange current density, pseudoequilibrium potential and anodic passive dissolution current) for rebars and anode elements, and the effective concrete resistances.

Selection of Model Polarization Parameters

To obtain the cathodic rebar polarization parameters, the rebar potentials and current values for all rebars in the chloride-free zone during a test interval were used to build a combined E-Log I graph. Figure 6 shows the combined cathodic polarization data and the corresponding abstracted curve for modeling. The shape of the plot suggests that most of the segments were under activation polarization control, so a cathodic Tafel slope, a pseudo exchange current (Ioc) and effective equilibrium potential (Eoc), were calculated to match the observed data shown in this figure. A constant passive current Ip was used as a constraint to fit the results to the observed potential values near zero current. The effective concrete resistance between consecutive rebar segments i and i+1 was designated R_{ci} and chosen to match the measured values in the same testing interval. The anodic Tafel slope for the rebar elements was given a nominal value of 60 mV.

Corresponding polarization data for anodic reaction in concrete slabs for initial modeling were not available. A simple activation polarization curve (E-log i) was considered for the model. The model parameters for the anodic reaction were quantified from the average of potentials and output macrocell currents obtained for the same test interval as used to evaluate the cathodic polarization parameters. For convenience an anodic Tafel slope of 0.45V was chosen for the predictive numerical model. The parameters for the anodic and cathodic components used as input data are shown in Table 2. A proposed method to identify the parameters characterizing the anodic polarization curve is presented later in this paper.

Modeling Cases

Two different cases were considered in the quantitative model. In the first case all rebars were connected, eight steel segments (#1-5 and #10-12) acting as simple cathodes under activation polarization control and four steel segments (#6 - 9) acting as combined anodic-cathodic elements. The second case replicated the condition after disconnecting the active rebars and had eight segments acting as simple cathodes and the rest in place but disconnected from the anode. In both cases, the anode was located between rebars 4 and 5 acting as a simple anodic element.

The predictive model was based in two principal assumptions: The sum of the potentials for each of the closed loops in the equivalent circuit and the sum of all anodic and cathodic currents was assumed to be equal to zero. The resulting system of equations was solved

numerically to obtain the yielding potentials for each node (E_1 to E_{12} and E_{Anode}), and the corresponding polarization current I_{ci} (I_{c1} to I_{c12} and I_{Anode}), which constituted the model output. I_{ci} designates the current associated with rebar segment i and E_1 to E_{12} represents the potential difference across the metal-concrete interface.

The equation for each node in the equivalent circuit of Figure 5 was established as:

$$E_i = E_{i+1} + Rc_i \cdot \sum_{1}^{i} I_i \qquad (1)$$

For purely cathodic or purely anodic polarization the equation for the segment i was:

For a purely cathodic bar:

$$E_i = Ec_i + \beta c_i \cdot \log\left(\frac{Is_i + I_P}{Ic_i}\right) = f_C(Is_i) \qquad (2)$$

For a purely anodic bar:

$$E_i = Ea_i + \beta a_i \cdot \log\left(\frac{Is_i}{Ia_i}\right) = f_a(Is_i) \qquad (3)$$

The general node equation becomes:

$$f_{a,c}(I_i) = f_{a,c}(I_i) + Rc_i \cdot \sum_{1}^{i} Is_i \qquad (4)$$

For the application case of rebars with mixed anodic-cathodic behavior, the segment was assumed to consist of two consecutive nodes, one as a cathodic and the other as an anodic element. The resistance between these two nodes was a nominal value (R = 1Ω) much smaller than the concrete resistance measured between elements.

Modeling Expansion Parameters

Efforts to experimentally characterize anode polarization

Long-Term in Situ Polarization Test*:* A long term polarization test was performed to obtain actual polarization parameters for the anodic component, to be used in the next generation modeling approach. The anode and rebar assembly were coupled through an external resistor of a known value. Six different resistance values, 500, 1k, 2k, 5k, 10k and 30k ohms were used in this test. An average five days data acquisition period was used after each resistor change, for a total evaluation period of approx. 62 days. External connections between the anode, resistors and rebar assembly, which were normally interconnected by

switches, allowed performing instant-off potential and current measurements of the anode during the test. The temperature was also recorded.

The polarization curves for the anode have been constructed using the current and potential values monitored at different times during the test period, following the installation of individual resistors. After testing with the largest (~ 30k ohm) resistor was completed, an infinite resistance condition corresponding to the open circuit condition (anode disconnected) was applied as well.

The resulting E- log I curves are illustrated in Figures 7a and 7b for each of the triplicate individual slab specimens of each anode type. For the C anodes the polarization curves in the forward and return directions in any given specimen matched well with little indication of hysteresis. The W anodes had aged significantly by the time of this test and showed on average much lower currents than those of the C anodes, but distinctly increased currents in the return than in the forward scan. That was especially the case for the W anode in slab 6, which tended to show somewhat erratic behavior over the long term (Figure 2).

The polarization curves deviate significantly from simple E-log I activation polarization behavior, and did not show a recognizable Tafel slope. The shape of the curves is suggestive of the presence of a very large ohmic polarization component. However, the ohmic explanation is not likely as the typical ohmic resistance as determined from instant-off and *ac* resistance measurements that were only in the order of 100 ohm, which could not explain the very large curvature observed. Thus, it appears that the polarization of the anodes is affected by a phenomenon akin to concentration polarization where the activity of substances accumulating at or near the anode metal surface varies with current. This possibility will be explored in subsequent work. Regardless of the shape, the curves show large specimen-to-specimen variability within a given group both in the anode open circuit potential and in the extent of current available when deviating from that potential.

Results from Controlled Humidity Chambers

Results from long-term polarization performance of galvanic point anodes in laboratory controlled humidity chambers under galvanostatic regime[5] are presented in figure 8. Comparison of polarization curves from high humidity chambers and the slabs tests are presented in Figure 9.

The E-Log I curve from humidity chamber tests showed comparable trends to those obtained in the slab tests as to shape of the polarization curve, but underscore the variability of the results specimens in the slabs.

Comparison of experimental results and modeling abstraction

Figure 9 also includes the anodic polarization curve used for the model calculations. The abstraction curve matches only roughly the ever increasing slope encountered experimentally. However, the systematic deviation incurred by the abstraction is still less than the observed variability between samples found so far and the fit provides a working approximation to observed behavior. Highly variable polarization response was observed from sample to sample. Additional experiments in progress will provide a statistical basis for

optimizing the abstraction, and determining the adequate degree of modeling complexity needed.

Long-Term in Situ Polarization Test - Fresh Anodes

Additional polarization data were obtained from a newly introduced (day 1050) set of fresh anodes of each type. These anodes were installed one bar spacing away from the initial anode position in the same concrete slabs as described in previous section, embedded in holes drilled in the slabs and filled with mortar. After 1 month stabilization with the new anodes replacing the previous set, another in-situ polarization test was performed using the same methodology as before, but over a period of only 10 days. The average results of triplicate specimens are summarized in the Figure 10 for both C and W anodes. The new anodes showed, as expected, greater current delivery at comparable potentials. Notably the fresh W anodes showed much lower polarization than the fresh C anodes, but from a more positive starting potential. Comparison of polarization curves from individual anodes (to be reported in subsequent publications) showed, for the fresh C anodes, unit to unit sample variability comparable to that observed earlier. The unit to unit variability suggests that performance predictions as needed for future model applications will require a statistical approach.

RESULTS AND DISCUSSION

Initial results show that the simplified one-dimensional approach used replicates major trends of the modeling condition including cathodic polarization potentials as function of distance on each side of the active rebars and the general magnitude of the currents and potentials observed there. The following exemplifies observations and modeling of the behavior of the C type anodes.

Figure 11 shows the model output and corresponding experimental data for the period between days 195 and 477 when all rebars were interconnected. Clearly the active bars in the high chloride zone are the main contributors to the anodic current, of the same order as the current delivered by the anode. Note that the operating potential of the anode is modest (~ -350 mV CSE), reflecting significant polarization of the anode noted in related work [5]. The model closely emulates the observed current distribution pattern and the measured potential trends. The polarization decay in the passive assembly with increasing distance from the anodic elements and the point anode is distinctly observed and reproduced by the model. The main effect is the decrease on the cathode currents with increasing distance from the anode.

Figure 12 addresses a later period (days 478 to 660) for the condition in which only passive rebars are allowed to interact with the point anode (the active rebars have zero current and their potentials are not shown). A reasonable agreement between modeled and experimental magnitudes was found. The anode is now the only source of polarization of the passive rebars, and makes up for some of the current that was delivered by the active bars in the previous example. Again the anode has been polarized to a modest operating potential. The model approaches well the experimental values also in this case; it is noted that this is achieved with the same polarization parameters for the bars used in the previous case without need to resort to customized parameter fitting. In both examples the concrete resistivity values (and associated resistances) were those measured for the test period emulated. Generic

resistivity values would be used in predictive cases as those considered in the next paragraph.

For both simulated conditions the model developed easily converging solutions and accurate balance between anodic and cathodic currents. The simple one-dimensional approach yielded usable approximations to the experimental observations and is easily scalable to a broader set of circumstances, as has been shown in previous work on computations of cathodic prevention patterns with a comparable approach [6]. Using a group of nominal parameters (geometrical configuration, resistivity values and polarization curves of the anode and cathode), this simplified model may be used to explore the effect of an anode specific type and location in the polarization distribution in a concrete- reinforcing steel system simulating a patch concrete repair situation. In particular, the model can be applied to estimating the number of anodes per unit length in a repair patch perimeter, needed to obtain a desired protective throwing power. This is addressed by increasing the length of the rebar segments or reducing the inter-segment distance to match a given steel placement density. Ongoing work on this application will be reported in a following paper.

CONCLUSIONS

1. A one-dimensional modeling approach using polarization data derived from test yard observations yielded workable approximations of the current and potential distribution in an actual system.

2. The model can be easily modified to address throwing power and anode performance in conditions with varying steel and anode placement densities.

3. Polarization experiments with both test yard slabs and environmental chamber specimens revealed polarization curves of similar shape but also show large sample to sample variability. The present modeling abstraction curve represents a working approximation subject to improvement as additional data become available. Future modeling improvement should use a statistical approach to define polarization parameters.

ACKNOWLEDGEMENTS

This investigation was supported by the State of Florida Department of Transportation and the U.S. Department of Transportation. The opinions, findings and conclusions expressed in this publication are those of the authors and not necessarily those of the supporting agencies.

REFERENCES

1. J. Bennett and C. Talbot, “Extending the Life of Concrete Patch Repair with Chemically Enhanced Zinc Anodes”, Paper No. 02255, Corrosion/2002, NACE International, Houston, 2002.

2. G. Sergi and C. Page, "Sacrificial anodes for cathodic prevention of reinforcing steel around patch repairs applied to chloride-contaminated concrete". In: Mietz, J. et al (eds.), Corrosion of Reinforcement in Concrete, IOM Communications, London, European Federation of Corrosion Publications, No. 31, p.93-100, 2001.

3. D. Whitmore and S. Abbott, “Using Humectants to Enhance the Performance of Embedded Galvanic Anodes”, Paper No. 03301, Corrosion/2003, NACE International, Houston, 2003.

4. J. Bennett and W. McCord, “Performance of Zinc Anodes Used to Extend the Life of Concrete Patch Repairs”, Paper No. 06331, Corrosion/2006, NACE International, Houston, 2006.

5. M. Dugarte, A.A. Sagüés, R. G. Powers and I. R. Lasa, “Evaluation Of Point Anodes For Corrosion Prevention In Reinforced Concrete”, Paper No. 07304, Corrosion/2007, NACE International, Houston, 2007.

6. F.J Presuel Moreno, S.C. Kranc, and Sagüés, A. A., “Cathodic Prevention Distribution in partially Submerged Reinforced Concrete”, Corr. Sci. Vol. 45 p.25-30 (2003).

7. Sagüés, A. A., Pech-Canul, M.A., and Al-Mansur, A.K.M. “Corrosion macrocell behavior of reinforcing steel in partially submerged concrete columns”, Corr. Sci. Vol. 61 p.548-558 (June 2005).

TABLE 1
MATERIALS AND TEST CONDITIONS

Anodes evaluated	C and W
Embedding media	Ordinary Repair Concrete (ORC): 0.41 w/c, 658 pcy (390.38 Kg/m^3), Type II cement, 3/8” Aggregates. Shaded portion near the center (Figure 1) - 6 Kg/m^3 chloride ion
Replication	Triplicate
Total test Slabs	6

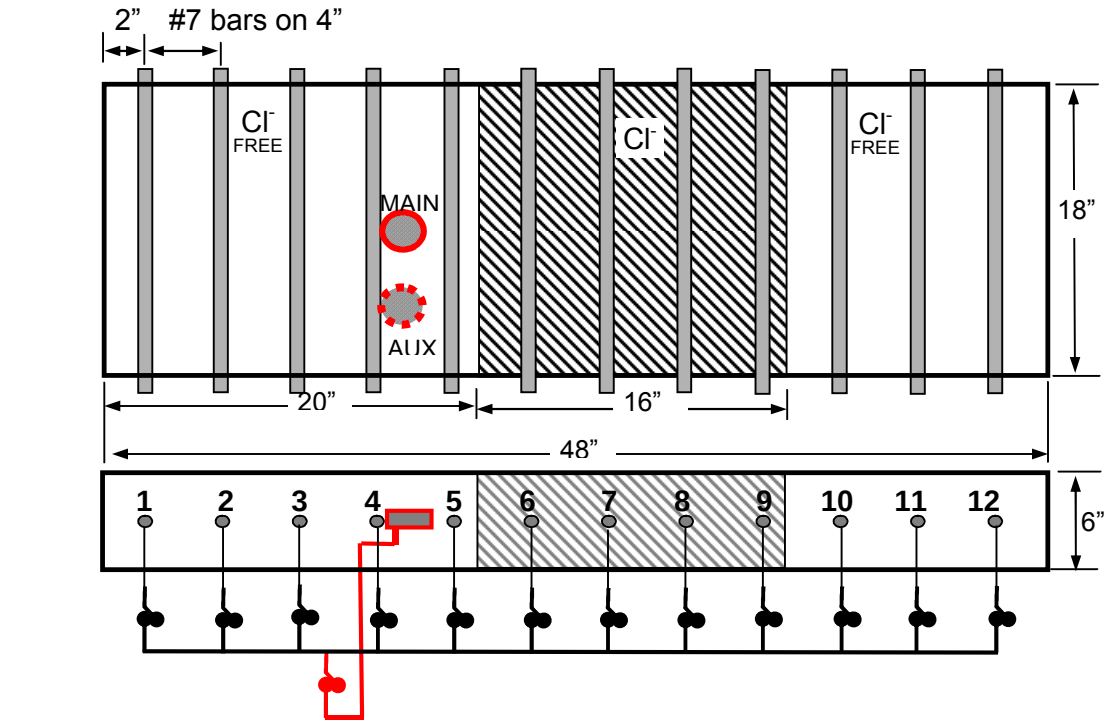

FIGURE 1- Test Slab Configuration. Plan and elevation view. 1” = 2.54 cm

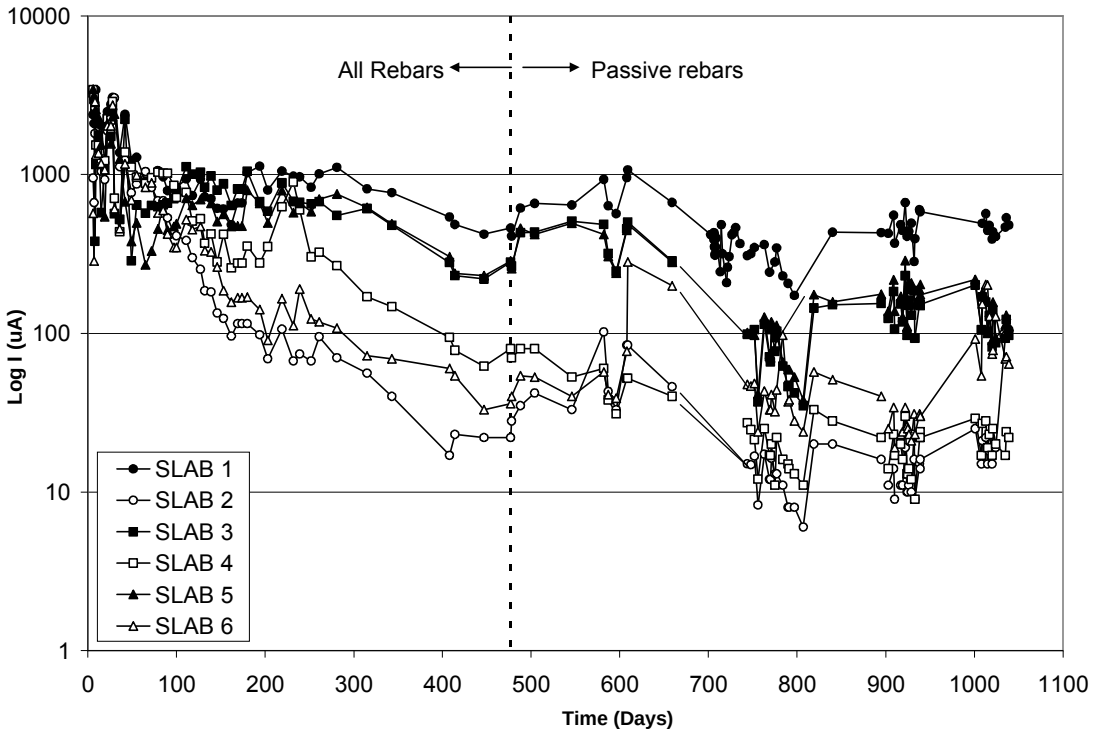

FIGURE 2 - Main anode current as function of exposure time. Slabs 1, 3, 5: C anode. Slabs 2, 4, 6: W anode

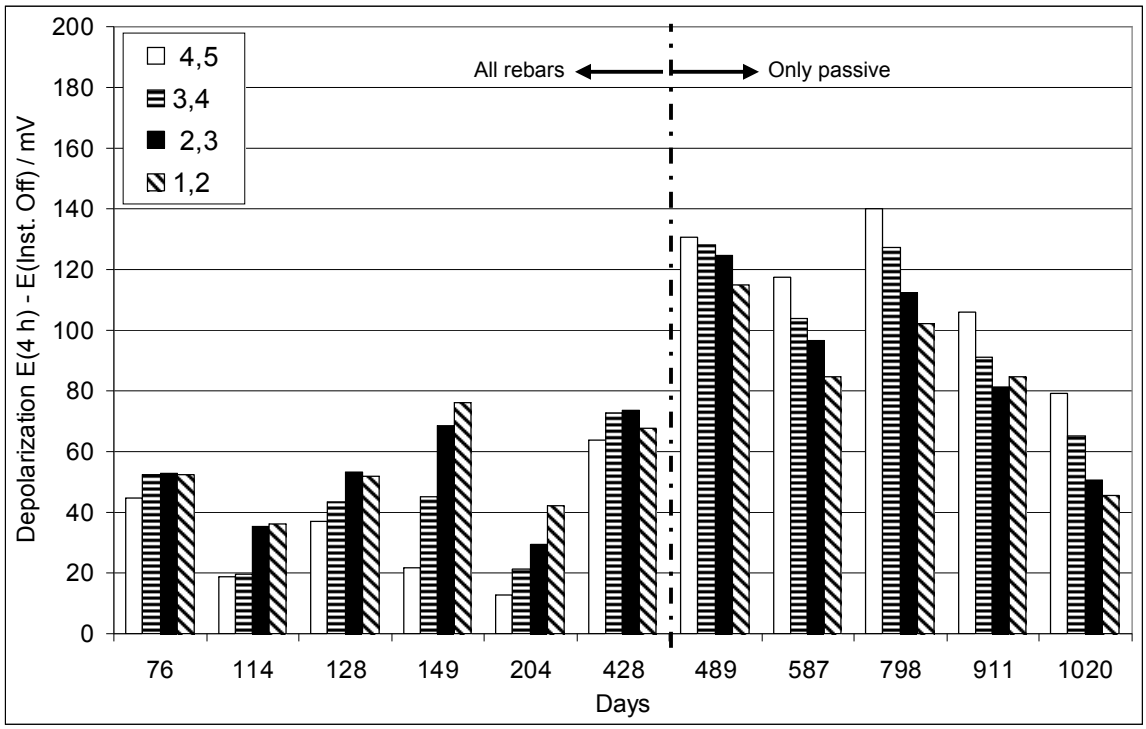

FIGURE 3 - Four-hour rebar depolarization test of C anode.
Average results of triplicate slabs.

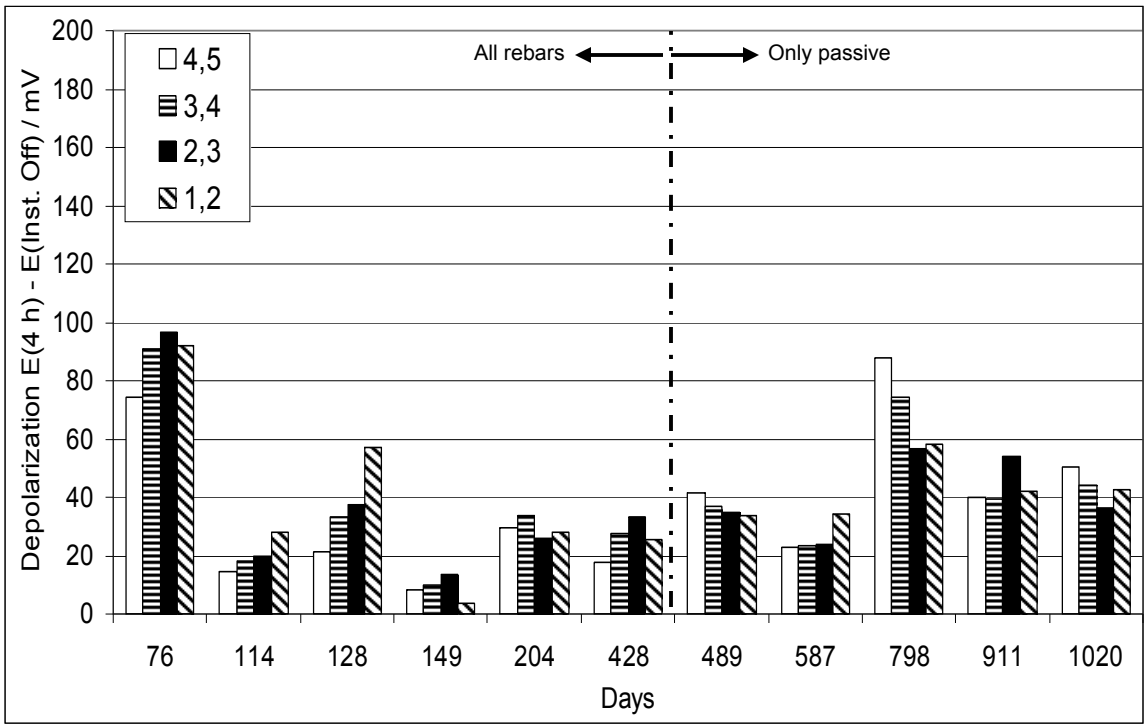

FIGURE 4 - Four-hour rebar depolarization test of W anodes.
Average results of triplicate slabs.

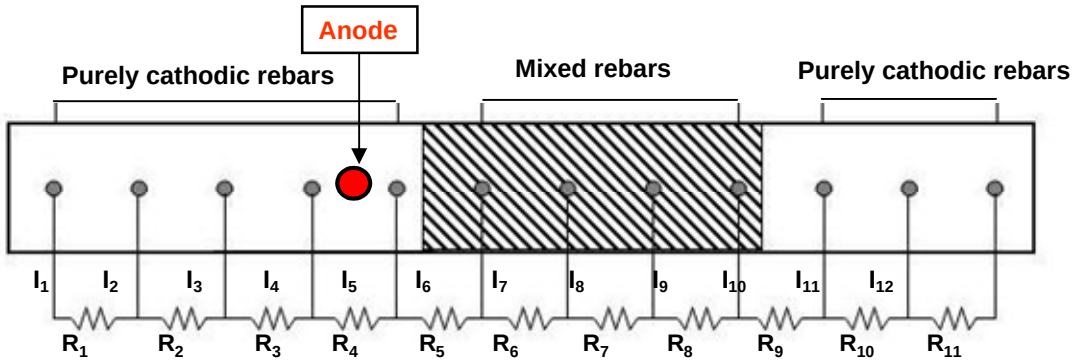

FIGURE 5- Electrical Equivalent Circuit

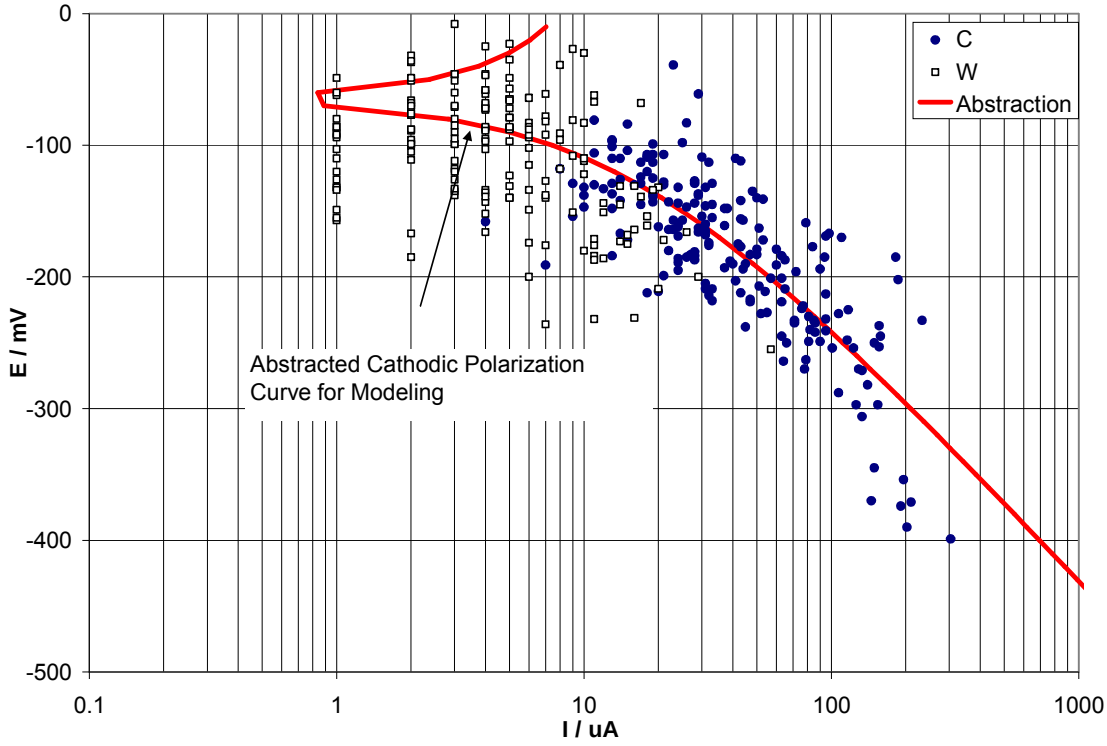

FIGURE 6 - Combined cathodic polarization data from all passive rebars in test slabs. Test period of 180 days.

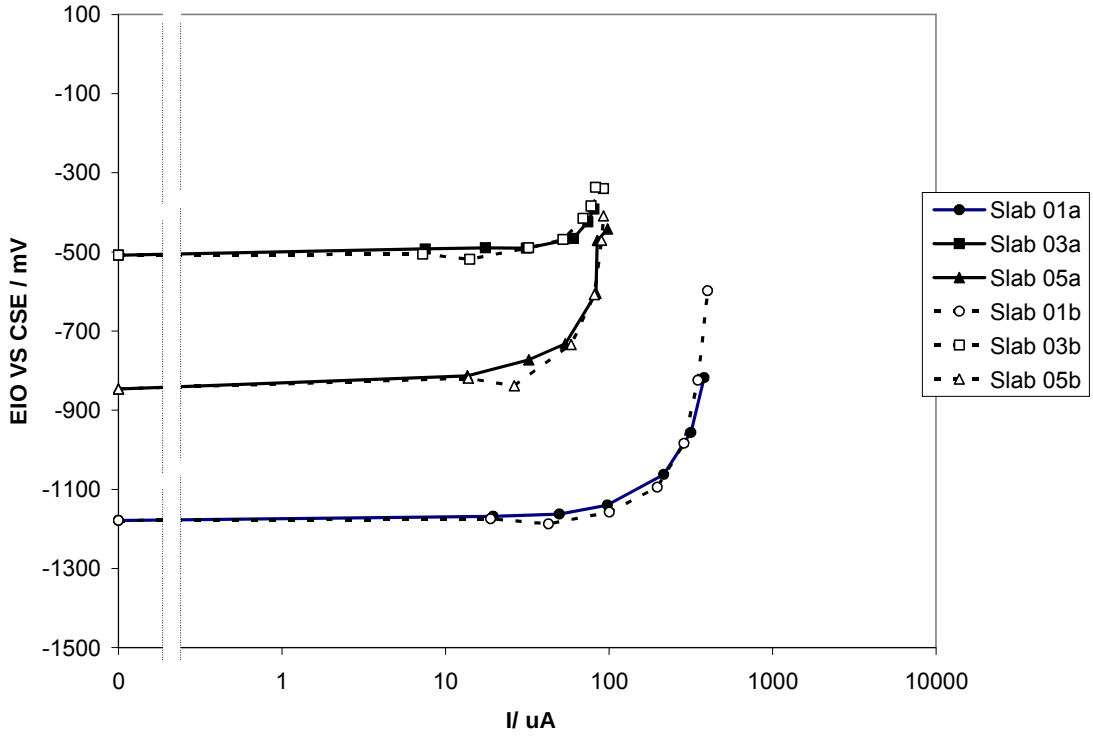

FIGURE 7a - E_{IO}-log I curves of C anodes in Slabs Test. Polarization curves in the forward (a) and return directions (b).

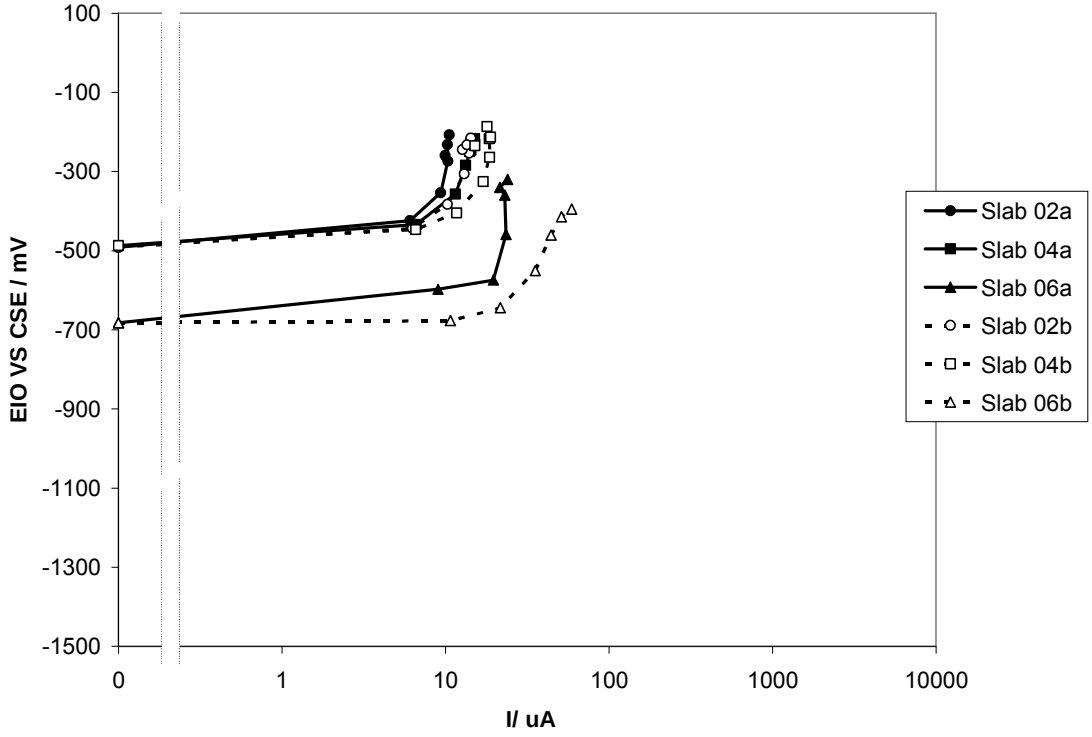

FIGURE 7b - E_{IO}-log I curves of W anodes in Slab Test. Polarization curves in the forward (a) and return directions (b).

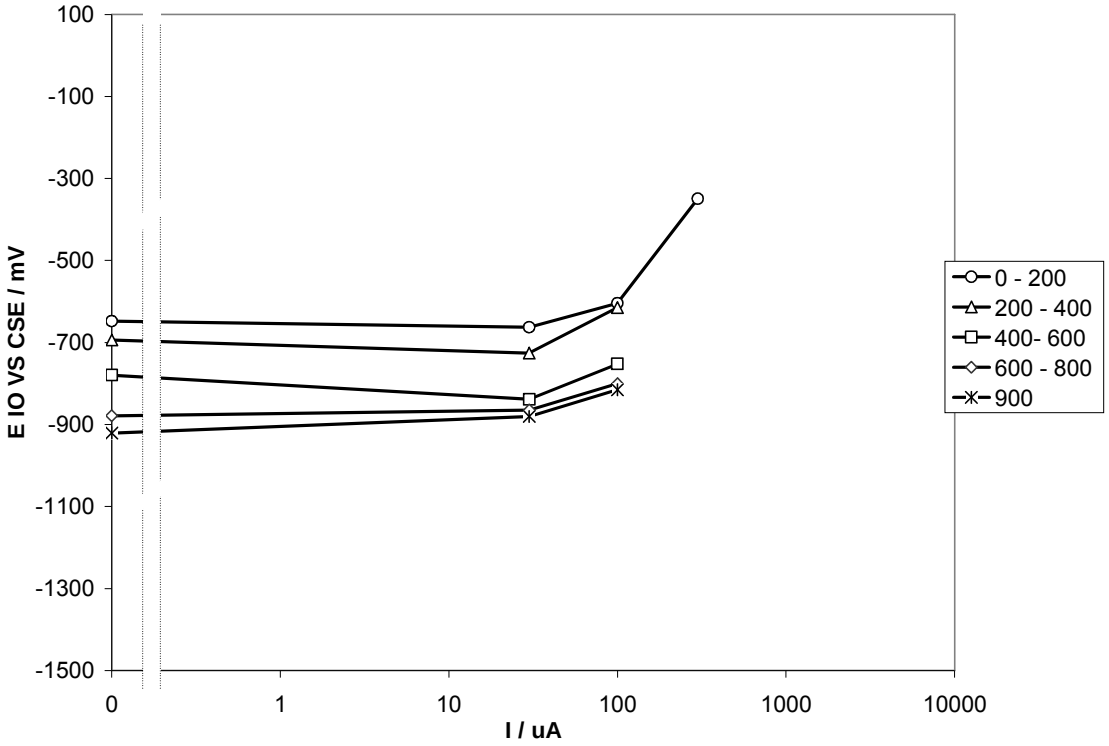

FIGURE 8 - E_{IO}-Log I evolution of C anode in the 95% R.H. test chamber. Averages for time periods shown in days since energizing

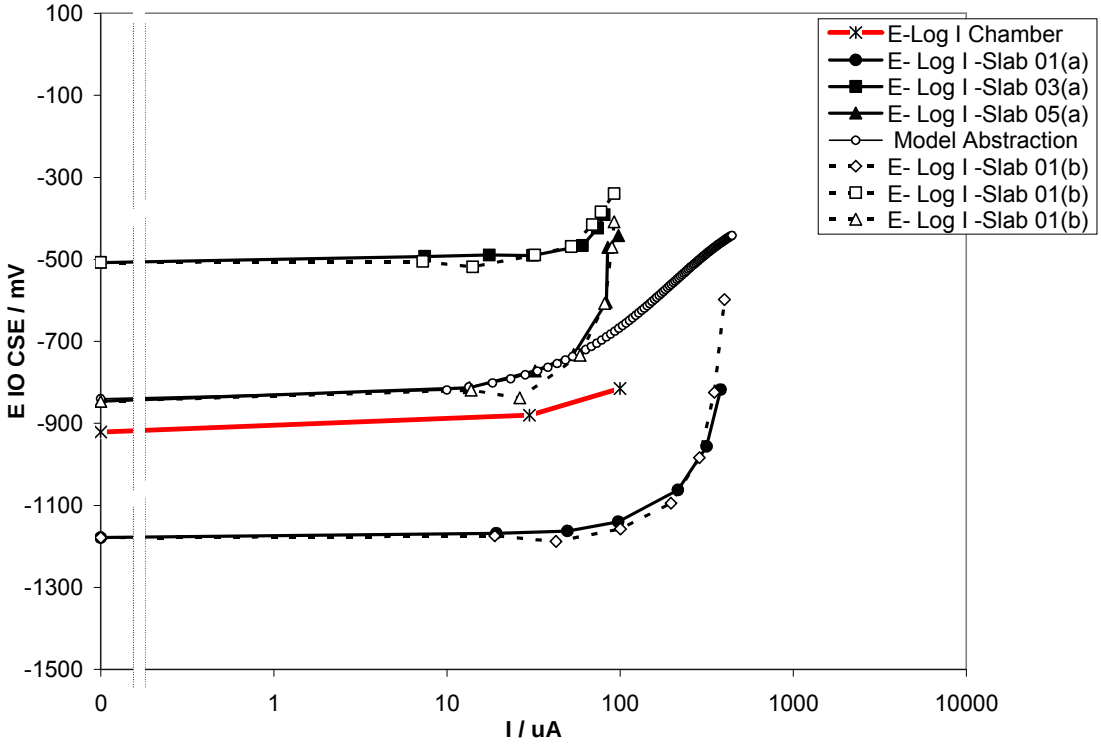

FIGURE 9 - Comparison between E_{IO}-I evolution of C anode from 95% R.H. test chamber (~900 days) and polarization curves from Slabs test (forward [a] and return [b]), with Model Abstracted polarization curve.

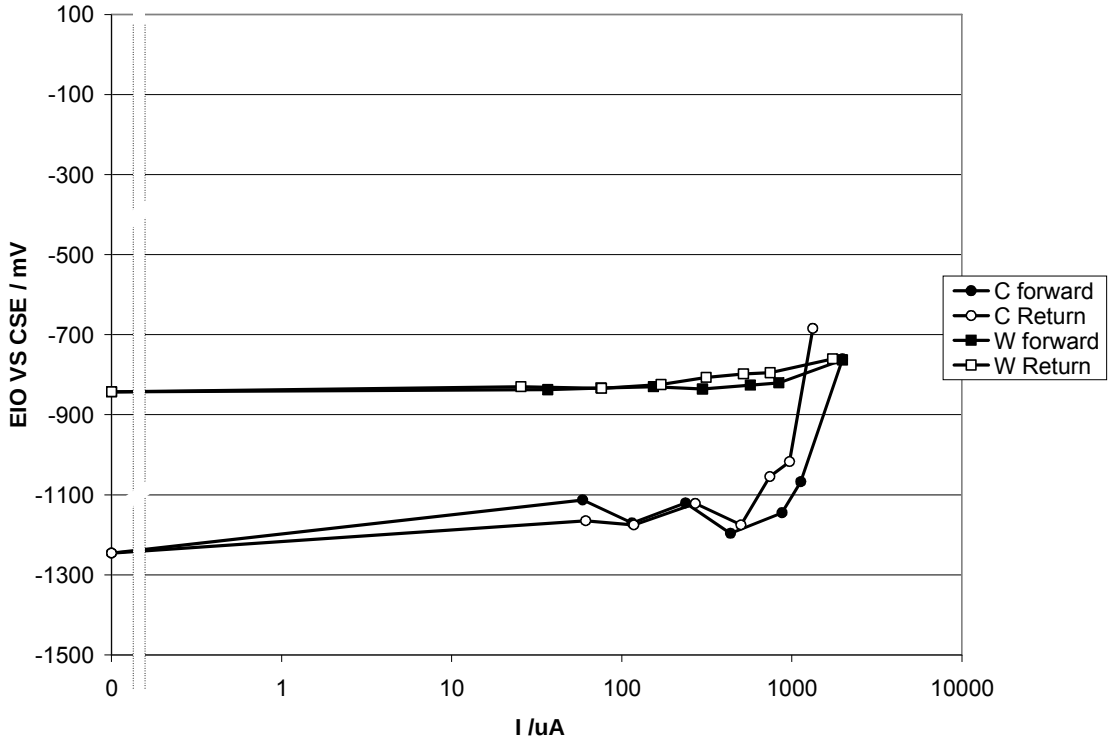

FIGURE 10 - E_{IO}-log I curves (forward and return) of fresh C and W anodes in Slab Tests. Average of triplicates.

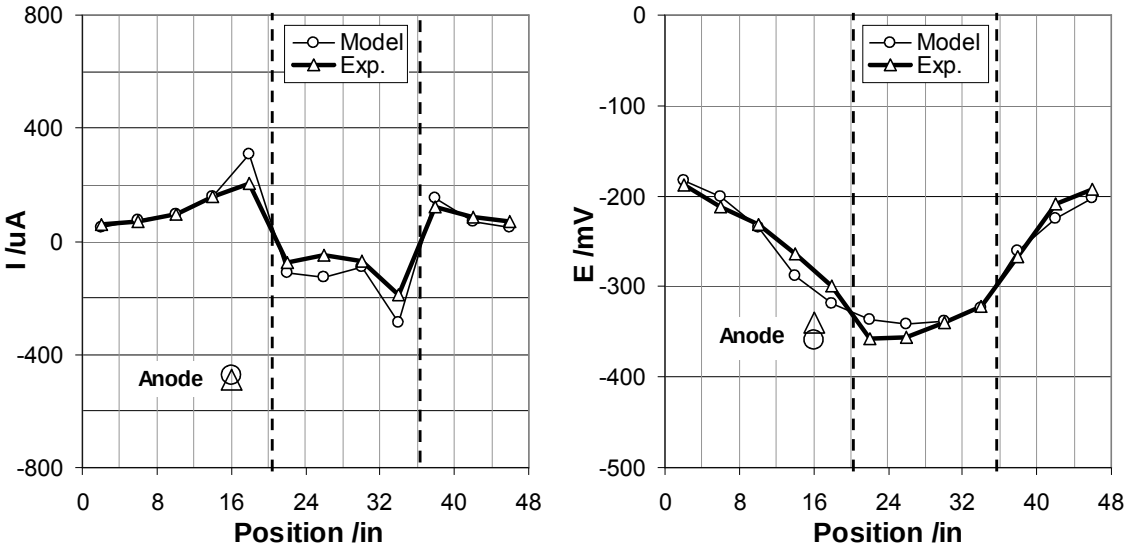

FIGURE 11 - Comparison between the model predicted values and the measured values of currents and potentials (Exp.). All rebars connected. Chloride contaminated portion indicated between vertical dotted lines.

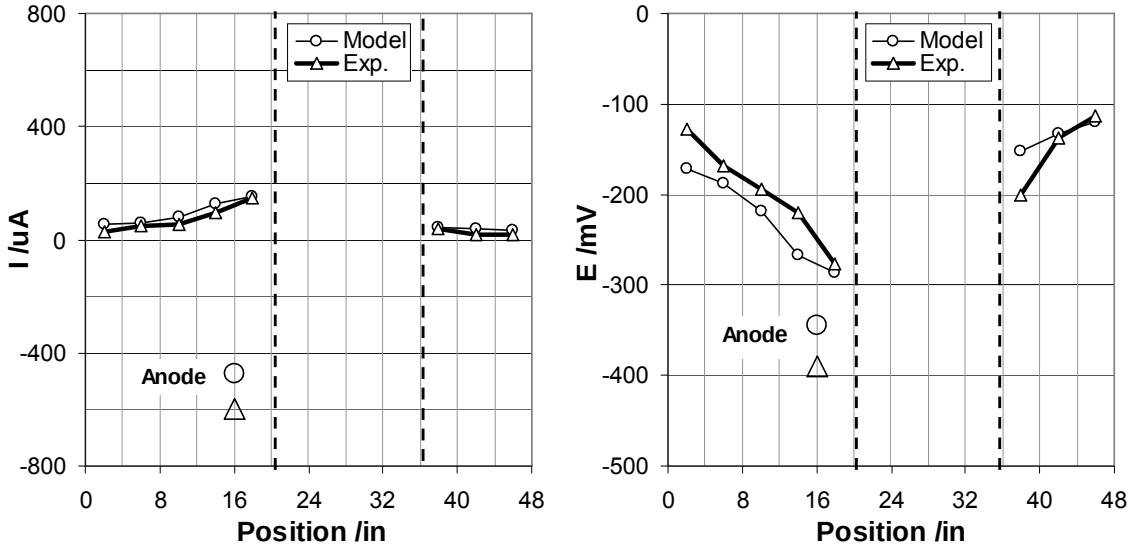

FIGURE 12- Comparison between the model predicted values and the measured values of currents and Potentials (Exp.). Rebars in the chloride contaminated zone disconnected from the anode assembly.

TABLE 2
INPUT PARAMETER VALUES FOR THE MODEL*

Case 1: All Rebars Connected		Case 2: Rebars (#6 - #9) disconnected	
Parameter	Purely Cathodic Rebars	Parameter	Purely Cathodic Rebars
Eoc (V) Ioc (A) βc (V)	-0.065 20×10^{-6} -0.250	Eoc (V) Ioc (A) βc (V)	-0.065 20×10^{-6} -0.250
Parameter	Point Anode	Parameter	Point Anode
Eoa (V) Ioa (A) βa (V)	-0.331 -0.564×10^{-3} 0.450	Eoa (V) Ioa (A) βa (V)	-0.390 -0.472×10^{-3} 0.450
Parameter	Mixed Rebars	N/A	N/A
Eocm / Eoam (V) Iocm / Ioam (A) βcm (V) βam (V)	-0.350 100×10^{-6} -0.250 0.060		

*Concrete resistance between segments matched measured values, typically 200 ohms/segment.